

Laser-assisted collision effect on nonsequential double ionization of helium in a few-cycle laser pulse

Hongyun Li^{1,2}, J. Chen³, Hongbing Jiang², Jie Liu³, Panming Fu¹, Qihuang Gong², Zong-Chao Yan^{4,5} and Bingbing Wang^{1*}

¹*Laboratory of Optical Physics, Beijing National Laboratory for Condensed Matter Physics, Institute of Physics, Chinese Academy of Sciences, Beijing 100080, China*

²*Department of Physics, State Key Laboratory for Artificial Microstructures and Mesoscopic Physics, Peking University, Beijing 100871, China*

³*Center for Nonlinear Studies, Institute of Applied Physics and Computational Mathematics, Beijing 100088, China*

⁴*Department of Physics, University of New Brunswick, P. O. Box 4400, Fredericton, New Brunswick, Canada E3B 5A3 and*

⁵*Center for Theoretical Atomic and Molecular Physics, the Academy of Fundamental and Interdisciplinary Sciences, Harbin Institute of Technology, Harbin 150080, China*

Abstract

Nonsequential double ionization (NSDI) of helium in an intense few-cycle laser pulse is investigated by applying the three-dimensional semi-classical re-scattering method. It is found that the momentum distribution of He^{2+} shows a single-double-single peak structure as the pulse intensity increases. According to the different mechanisms dominating the NSDI process, the laser intensity can be classified into three regimes where the momentum distribution of He^{2+} exhibits different characteristics. In the relatively high intensity regime, an NSDI mechanism named the “laser-assisted collision ionization” is found to be dominating the NSDI process and causing the single peak structure. This result can shed light on the study of non-sequential ionization of a highly charged ion in a relatively intense laser pulse.

* Corresponding author: wbb@aphy.iphy.ac.cn

I. INTRODUCTION

Study of non-sequential double ionization (NSDI) of an atom in a laser field has become an important research topic in strong-field physics [1, 2, 3, 4] since its first experimental observation in 1983 [5]. An NSDI process in an external laser field provides us with an effective way to investigate and eventually control the electron-electron correlations in a multi-electron atom or molecule experimentally [1, 2, 3] or theoretically [4, 6, 7, 8, 9]. At present, the widely accepted theory of NSDI is the three-step re-collision model [10, 11, 12], in which one electron first escapes from the atom by tunneling through the atomic-ground-state barrier, formed by the Coulomb potential and the laser field. It is then driven back by the laser field and collides with its parent ion, resulting in ionization or excitation of a second electron. According to this model, if the second electron is ionized directly by a collision with the returning electron, the process is called the collision-ionization (CI). Whereas if the second electron is excited by a collision followed by an ionization in the laser field through tunneling, the process is called the collision-excitation-ionization (CEI). It is now clear that when the laser intensity is so weak that the maximum returning kinetic energy $E_{\text{kin}}^{\text{max}}$ is smaller than the ionization potential of the second electron I_p [13], the NSDI process is dominated by the CEI mechanism, and the momentum distribution of the double charged ion along the polarization of the laser field shows a single peak at around the zero momentum. On the other hand, when the intensity increases so that $E_{\text{kin}}^{\text{max}}$ is larger than I_p , the NSDI is dominated by the CI mechanism, and the momentum distribution shows a double-peak structure with a minimum at the zero momentum. The distance between the two peaks increases as the intensity increases, and the extreme position of the right (left) peak is predicted to be $4\sqrt{U_p}$ ($-4\sqrt{U_p}$) [14], where U_p is the ponderomotive energy of the electron in the laser field. However, as the laser intensity further increases, whether or not the positions of the two peaks can remain is still an open question. Using the classical rescattering model, Feuerstein *et al.* [14] predicted that these two peaks will remain at the extreme values $\pm 4\sqrt{U_p}$ for double ionization and the momentum distribution of the multiple ionization will exhibit a broad distribution with multiple peaks at $\pm 2n\sqrt{U_p}$, where n is the number of the ionized electrons. However, the recent experimental observation by

Rudenko *et al.* [15] proved that the two peaks shifts towards considerably lower values as the intensity increases, and the distribution becomes a broader peak before the sequential ionization occurs. Obviously, these experimental results can not be simply attributed to the well-known CI mechanism.

In this work, we employ three-dimensional semi-classical re-scattering method [8, 9] to investigate the intensity dependence of the NSDI of helium in a few-cycle laser pulse. The momentum distribution exhibits a single-double-single peak structure as the intensity increases. In particular, a single peak distribution at a weak laser intensity becomes a double-peak structure and the positions of the two peaks increase to $\pm 4\sqrt{U_p}$ as the intensity increases. When the intensity increases further, the positions of the double peaks shift towards zero from $\pm 4\sqrt{U_p}$ and the two peaks finally become a single peak. These results agree qualitatively well with the experimental observations by Weber *et al.* [17] and Herrwerth *et al.* [18] (Fig. 4 in that paper) for doubly charged argon ions, as well as the results by Rudenko *et al.* for neon ions [15, 16]. Furthermore, through tracing the NSDI trajectories, we find that, when the intensity increases from intermediate- to strong-field regime, the NSDI mechanism changes from CI to a new mechanism which we call the “laser-assisted-collision-ionization” (LACI). In the strong-field regime, the trajectories with small energy transition between the two electrons during collision play a dominant role in the NSDI with the help of the laser field, leading to the single peak distribution. Our results can shed light on the study of non-sequential ionization of the highly charged ions in a relatively strong laser field.

The paper is organized as follows. In Sec. II, we will briefly review the basic theory of the three-dimensional semi-classical re-scattering method. In Sec. III, we will study the NSDI in different intensity regimes. In Sec. V, we will present the conclusions.

II. FORMULATION

We study the NSDI of helium in a linearly polarized few-cycle laser pulse. A more detailed description of the three-dimensional semi-classical recollision method may be found in [8, 9]. Here we briefly outline the formalism. Atomic units are used throughout, unless otherwise specified. The linearly polarized pulse is given by $\mathbf{E}(t) = -d\mathbf{A}(t)/dt$, where the vector potential is

$$\mathbf{A}(t) = (0, 0, A_0 \cos^2(\omega t/T) \sin(\omega t + \varphi_0)), \quad (1)$$

here ω is the carrier frequency, T is the pulse duration, and the carrier-envelope phase (CEP) of the pulse is $\varphi_0 = 0$ in the calculations. The first electron is set free by the external field with the weight given by the tunneling probability calculated using the Ammosov-Delone-Krainov (ADK) theory [19]. The subsequent evolutions of the ionized electron and the remaining bound electron, driven by the combined Coulomb potential and the laser field, are described by the classical Newtonian equation

$$\frac{d^2 \mathbf{r}_j}{dt^2} = -\mathbf{E}(t) - \nabla_j (V_{ne}^{(j)} + V_{ee}), \quad (2)$$

where $j = 1$ and 2 corresponding to the ionized and bound electron respectively. The Coulomb potential between the nucleus and the electron is $V_{ne}^{(j)} = -2/|\mathbf{r}_j|$, and the Coulomb potential between the two electrons is $V_{ee} = 1/|\mathbf{r}_1 - \mathbf{r}_2|$.

To evolve Eq. (2), we need to know the initial positions and velocities of the two electrons. The initial position of the ionized electron is determined by an equation which includes an effective potential [8, 9]. The initial velocity of this electron is set to be $v_x = v_{\text{per}} \cos \theta$, $v_y = v_{\text{per}} \sin \theta$, and $v_z = 0$. The initial conditions for the bound electron are determined by assuming that the bound electron is in the ground state of He^+ and its initial distribution obeys the micro-canonical distribution [20]. The weight of each classical trajectory is proportional to $W(t_0, v_{\text{per}}) = w(t_0)\bar{w}(t_0, v_{\text{per}})$, where $w(t_0)$ is the tunneling ionization probability at time t_0 given by the ADK theory and the quantum mechanical transverse velocity distribution [8, 9] of the ionized electron is

$$\bar{w}(t_0, v_{\text{per}}) = \frac{(2|I_p|)^{1/2}}{|\mathbf{E}(t_0)|\pi} \exp(-v_{\text{per}}^2 (2|I_p|)^{1/2} / |\mathbf{E}(t_0)|), \quad (3)$$

with I_p being the ionization threshold of Helium. This distribution is adopted to simulate the quantum diffusion of the ionized wave packet moving in the external field.

We choose a starting time t_0 , which is uniformly distributed along the whole pulse, and then evolve Eq. (2) to the end of the pulse. In order to find out whether both electrons are ionized, we calculate the final energy of each electron after that the laser pulse has been turned off. If both electrons have positive energies, then the NSDI has occurred. The frequency of the laser pulse is $\omega = 0.0578$ a.u. (the wavelength $\lambda = 760$ nm) and the pulse duration is $T = 13.5$ fs which contains five optical cycles. Figure 1 presents the ionization yield of He^{2+} ion as a function of the laser intensity. The well-known ‘‘shoulder structure’’ shown in Fig. 1 indicates that the laser intensity considered in this work is below the sequential double ionization threshold of helium.

III. INTENSITY DEPENDENCE OF NSDI IN A FEW-CYCLE PULSE

We now consider the intensity dependence of NSDI of a helium atom in a few-cycle pulse. Figure 2 presents the momentum distribution of He^{2+} parallel to the polarization of the laser field for the peak intensity $I = 2 \times 10^{14} \text{ W/cm}^2$ (a), $2.5 \times 10^{14} \text{ W/cm}^2$ (b), $3.5 \times 10^{14} \text{ W/cm}^2$ (c), $5.0 \times 10^{14} \text{ W/cm}^2$ (d), $7.0 \times 10^{14} \text{ W/cm}^2$ (e), and $1 \times 10^{15} \text{ W/cm}^2$ (f). The distribution shows a single-double-single peak structure as the intensity increases, hence we classify the laser intensity into three regimes, according to the characteristics of the momentum distribution of He^{2+} shown in Fig. 2. In the weak-field regime (Fig. 2(a)), there is a single peak centered at the $+|P_z|$ direction which is very close to zero momentum. In the intermediate-field regime (Figs. 2(b)-2(e)), a double-peak structure is formed and the distance between the two peaks changes with the intensity. The maximum (minimum) position of the right (left) peak is $4\sqrt{U_p}$ ($-4\sqrt{U_p}$) at $I = 3.5 \times 10^{14} \text{ W/cm}^2$. Finally in the strong-field regime (Fig. 2(f)), the momentum distribution presents a single peak.

According to the three-step recollision model, there are three factors which can influence the NSDI rate: (1) the tunneling rate of the first electron e_1 , (2) the kinetic energy that e_1 can carry when it returns, and (3) the influence of the laser field on the recollision process when e_1 returns. The relative role of these three factors in determining the NSDI yield can be identified by analyzing the momentum distribution of the He^{2+} ion. Furthermore, the crucial influencing factor on NSDI, as well as the corresponding mechanism, differs in different intensity regimes.

A. Weak- and intermediate-field regime

We first consider NSDI in the weak-field regime. It is well known that, when the intensity of the laser is so weak that the maximum kinetic energy of the returning electron is smaller than the ionization potential of He^+ , the CEI mechanism dominates the NSDI process, where there is an obvious time delay between the recollision of the first electron and the ionization of the second electron. We now perform a time-momentum analysis of the NSDI process [18] to illustrate the NSDI in such a weak laser field. Figure 3(a) presents the NSDI momentum distribution as a function of time when $I = 2 \times 10^{14} \text{ W/cm}^2$. The horizontal and vertical axes correspond to the time when NSDI occurs and the momentum of He^{2+} parallel to the

laser field. The dashed curve is the corresponding laser field. One can see that there is only one group of NSDI trajectories appearing at about 0.5 laser cycle where is one extreme of the laser field, as shown in Fig. 3(a). We then trace back these NSDI trajectories to the recollision time of the first electron as shown in Fig. 3(b), where the recollision time is defined as the moment that the collision between the two electrons happens. The horizontal and vertical axes correspond to the recollision time and the kinetic energy E_{kin} of the returning electron. Figure 3(b) shows that the maximum value of E_{kin} , which occurs at about 0.25 laser cycle, is smaller than the ionization potential of He^+ . Comparing Figs. 3(a) with 3(b), one can find that the time delay between the double ionization and recollision is about 1/4 laser cycle. Additionally, Fig. 3(b) shows that only the electron of large kinetic energy which returns at about 0.25 laser cycle contributes to the NSDI. This indicates that, in the weak-field regime, where the CEI dominates the NSDI process, the returning kinetic energy E_{kin} plays a crucial role in the NSDI yield.

We next consider the NSDI in the intermediate-field regime where the momentum distribution of the He^{2+} ion displays a double-hump structure. From Fig. 2 one can see that this double-hump structure is well preserved over a large range of the laser intensity, which qualitatively agrees with the COLTRIMS neon data of Ullrich group [21]. Specifically, the intensity region is from $2.5 \times 10^{14} \text{ W/cm}^2$ to $8 \times 10^{14} \text{ W/cm}^2$ in our calculations.

Similar as Fig. 3(a), Figure 4(a) illustrates the momentum distribution of the He^{2+} ion as a function of the NSDI time with $I = 3.5 \times 10^{14} \text{ W/cm}^2$. For comparison, the laser field $E(t)$ is also presented (the dashed curve). Figure 4(a) shows that there are four groups of NSDI trajectories where the double ionization (DI) occurs at approximately 0.2, 0.5, 0.7, and 1.0 laser cycle. Tracing back to the recollision time of the first electron for these trajectories, we find that there are two bunches of recollision trajectories corresponding to the four groups of the DI trajectories, which is labeled by BI and BII in Fig. 4(b). Furthermore, we find that the first and second groups of the NSDI trajectories in Fig. 4(a) come from BI and the third and fourth groups come from BII. The double ionization of the first and third groups in Fig. 4(a) occurs at about the zero crossings of the laser field (0.2 and 0.7 laser cycle, respectively), with almost no time delay comparing with the corresponding recollision time of e_1 . Obviously, this NSDI process is CI process. In contrast, the second and fourth groups of NSDI trajectories occur at about the maximum (minimum) of the laser cycles with a time delay of about 1/4 laser cycle between the DI and the recollision, indicating that these two

groups are CEI process. Moreover, the first and third groups of NSDI trajectories dominate the contribution to NSDI, leading to a double peak structure in the momentum distribution of He^{2+} (Fig. 2(c)).

In the intermediate-field regime as shown in Fig. 4, since the maximum values of the returning kinetic energy of e_1 for both bunches BI and BII are larger than the ionization potential of e_2 , the kinetic energy is no longer the most crucial factor to influence the NSDI yield. In contrast, the tunneling rate of e_1 plays the most important role in influencing the NSDI [22]. Consequently, the third group from BII, which experiences a larger tunneling rate, contributes more to the NSDI (Fig. 4(a)) than the first group from BI, resulting in that the left peak is higher than the right one in the momentum distribution in Fig. 2(c).

B. Intense-field regime

We then further increase the intensity and find that the two peaks of the momentum distribution merge into one peak when $I = 1 \times 10^{15} \text{ W/cm}^2$, as shown in Fig. 2 (f). We also present the momentum distribution of He^{2+} as a function of time for $I = 1 \times 10^{15} \text{ W/cm}^2$ in Fig. 5 (a). The dashed curve is the corresponding laser field. There are four groups of NSDI trajectories presented in Fig. 5(a). We also trace back these NSDI trajectories to the recollision time of e_1 . The kinetic energy distribution versus collision time is presented in Fig. 5(b). There are mainly three bunches of recollision trajectories, labeled as BI, BII, and BIII in Fig. 5(b). The other weak bunches, labeled as DI, DII, and DIII in Fig. 5(b), are from the multiple recollision and have neglectable contributions to NSDI. Comparing Figs. 5(a) with 5(b), we find that there is almost no time delay between the recollision of e_1 and the ionization of e_2 for the first three groups of the NSDI trajectories, whereas there is about 1/4 laser cycle delay time between the fourth group and the corresponding recollision bunch BIII. Furthermore, each one of the first three groups presents a wide distribution, while the main parts of the first two groups occur at about the maximum (minimum) of the laser cycles, as shown in Fig. 5 (a). Comparing these two groups with the first and third groups in Fig. 4(a), we find that these two groups can not be attributed to the usual CI mechanism. We hence define this new mechanism as the “laser-assisted collision ionization” (LACI). The difference between a CI and a LACI trajectory can be clarified as follows. For a CI trajectory, the first electron is ionized with a relatively lower tunneling rate (comparing

with a LACI trajectory), then it returns with a higher kinetic energy and collides with the second electron at about the zero-crossing of the laser field, where the influence of the laser on the recollision can be ignored, and the recollision process can roughly be treated as a field-free collision process [23]. In contrast, for a CI trajectory, the first electron is ionized with a relatively higher tunneling rate, then it returns with a relatively lower kinetic energy and finally collides with the second electron at about one extreme of the laser field, where the laser field strongly affects the collision process and assists the first electron to free the second electron. Furthermore, for a CI trajectory, because the second electron is ionized by collision at about the zero-crossing of the laser field, the final momentum of the He^{2+} ion is at about $\pm 4\sqrt{U_p}$ [14], as shown in Fig. 2 (c); In contrast, for a LACI trajectory, because the second electron is ionized by collision at the extreme of the laser field, the final momentum of He^{2+} ion is at around zero [14], as shown in Fig. 2 (f).

In order to demonstrate that the LACI mechanism plays a dominant role in leading to the single peak structure in the momentum distribution in the intense-field regime, we recalculate the NSDI at $I = 1 \times 10^{15}$ W/cm² by turning off the laser field during the collision between the returning e_1 and the ion for each NSDI trajectory. We turn off the laser field when the returning electron is within $r_1 = 5$ a.u. from its parent ion. In this way, we suppress the influence of the laser field on the recollision process when e_1 passes through the ion. In order to keep a small difference of the returning kinetic energy of e_1 for the two cases, we choose $r_1 = 5$ a.u. as the signal to turn off the laser. In fact, we have obtained the similar results when $r_1 = 10$ a.u. Figure 2(f) presents the momentum distribution with (the solid curve) and without (the dashed curve) the laser field during the recollision. It clearly shows that the contributions from the trajectories with small returning kinetic energy of e_1 are suppressed when the laser field is turned off during the collision, resulting in that the double-peak structure survives in such a high laser intensity. This result confirms that the LACI is the dominant NSDI mechanism in the intense-field regime and causes the single peak structure in the momentum distribution of He^{2+} . For comparison, we also present the momentum distribution without the laser field (the dashed curve) during the recollision for the case of $I = 7 \times 10^{14}$ W/cm² in Fig. 2(e) and $I = 3.5 \times 10^{14}$ W/cm² in Fig. 2(c). For both cases, the double peak structure remains when the laser field is turned off during the collision, although the NSDI yield decreases a little. It indicates that the influence of the laser field on the recollision process does not play a key role on the NSDI in the intermediate

laser intensity regime.

To investigate in detail how the laser field affects the NSDI yield through influencing the recollision process, we present two typical LACI trajectories in Figs. 6 and 7 for the recollision electron e_1 (a) and the bound electron e_2 (b). For comparison, Figs. 6(c) and 6(d) respectively show the corresponding trajectories of e_1 and e_2 without the laser field during the collision between the returning electron and the ion core. As shown in Fig. 6(c), one can see that without the help of the laser field, although the bound electron e_2 is set free by the collision, the returning electron e_1 is recaptured by the ion core; this is because that its small returning kinetic energy can not overcome the Coulomb force of the ion. Hence in this case, the laser field accelerates e_1 passing through the ion core to avoid the Coulomb recapture of the ion.

Figure 7 presents another kind of LACI trajectory for e_1 (a) and e_2 (b). Figs. 7(c) and 7(d) respectively show the corresponding trajectories of e_1 and e_2 without the laser field during the collision. As shown in Fig. 7(d), if the laser field is turned off, although e_1 passes through the ion core successfully, e_2 is still bounded by the ion core after the collision; this is because that the small energy transition can not set it free from the Coulomb bound state. Comparing Figs. 7(b) with 7(d), one can find that the acceleration along the z -axis by the laser field during the collision helps e_2 get rid of the binding of the ion. This can also be understood as that the laser field lowers down the Coulomb barrier of the ion along the z -axis during the collision, resulting in freeing e_2 after the collision.

These two kinds of LACI trajectories indicate that the influence of the laser field on the collision is twofold: on the one hand, the laser field accelerates e_1 during the collision to avoid the Coulomb recapture of the ion core; on the other hand, the laser field lowers down the Coulomb barrier of e_2 along the z -axis to provide it a chance to get free through the collision.

The experimental observation by Rudenko *et al.* [15] can be clearly explained by the LACI mechanism. As mentioned in [15], when the laser intensity is larger than 4×10^{15} W/cm², the main channel for the Ne³⁺ ion is the sequential ionization of the first two electrons e_1 and e_2 followed by the non-sequential ionization of the third electron e_3 by recollision of e_2 with the Ne²⁺ ion. In that intense-field regime, the laser accelerating effect on e_2 and the lower-barrier effect on e_3 during the recollision influence the NSDI trajectory effectively, leading to that the returning trajectory, which collides with the ion at the extreme of the

laser field, starts to provide more contributions and finally makes dominant contribution to the NSDI as the laser intensity increases. As a result, the double peaks of the Ne^{3+} ion in the momentum distribution shift towards each other and eventually merge into one peak as the intensity increases from $4 \times 10^{15} \text{ W/cm}^2$ to $7 \times 10^{15} \text{ W/cm}^2$ as shown in Fig. 1 of Ref. [15].

IV. CONCLUSIONS

In this paper, we have presented a systematic study of NSDI of helium in an intense few-cycle laser pulse by using the three-dimensional semi-classical re-scattering method. According to the different mechanisms dominating the NSDI process, the laser intensity can be classified into three regimes where the momentum distribution of He^{2+} exhibits different characteristics. In particular, the momentum distribution of He^{2+} shows a single-double-single peak structure as the pulse intensity increases. In the relatively high intensity regime, a new NSDI mechanism which is named the “laser-assisted collision ionization” is found to dominate the NSDI process and cause the single peak structure before the sequential ionization occurs. This result can explain the recent experimental observation of Rudenko *et al.* [15].

Acknowledgments

This research was supported by the National Natural Science Foundation of China under Grant Nos. 60778009, 10634020 and 10521002, 973 Research Projects No. 2006CB806000 and No. 2006CB806003. ZCY was supported by NSERC of Canada. BW thanks Jiangbin Gong for helpful discussions. HL thanks Xiaojun Liu for helpful discussions.

-
- [1] A. Staudte, C. Ruiz, M. Schöffler, S. Schössler, D. Zeidler, Th. Weber, M. Meckel, D. M. Villeneuve, P. B. Corkum, A. Becker, and R. Dörner, *Phys. Rev. Lett.* **99**, 263002 (2007).
 - [2] A. Rudenko, V. L. B. de Jesus, Th. Ergler, K. Zrost, B. Feuerstein, C. D. Schröter, R. Moshhammer, and J. Ullrich, *Phys. Rev. Lett.* **99**, 263003 (2007).

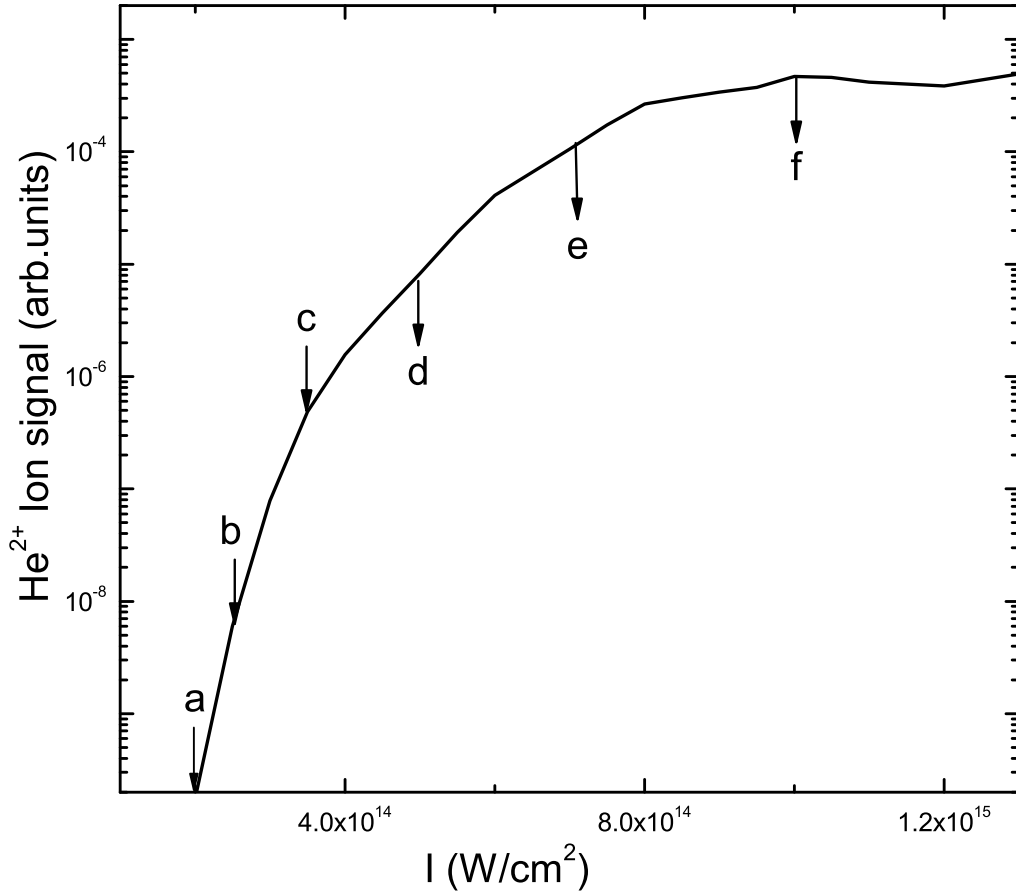


Figure 1: Yield of He^{2+} as a function of the peak intensity of the laser pulse with $\varphi_0 = 0$.

- [3] R. Panfili, S. L. Haan, and J. H. Eberly, Phys. Rev. Lett. **89**, 113001 (2002); S. L. Haan, P. S. Wheeler, R. Panfili, and J. H. Eberly, Phys. Rev. A **66**, 061402(R) (2002); P. J. Ho, R. Panfili, S. L. Haan, and J. H. Eberly, Phys. Rev. Lett. **94**, 093002 (2005); S. L. Haan, L. Breen, A. Karim, and J. H. Eberly, Phys. Rev. Lett. **97**, 103008 (2006); P. J. Ho, and J. H. Eberly, Phys. Rev. Lett. **97**, 083001 (2006).
- [4] X. Liu, H. Rottke, E. Eremina, W. Sandner, E. Goulielmakis, K. O. Keeffe, M. Lezius, F. Krausz, F. Lindner, M. G. Schätzel, G. G. Paulus, and H. Walther, Phys. Rev. Lett. **93**, 263001 (2004).

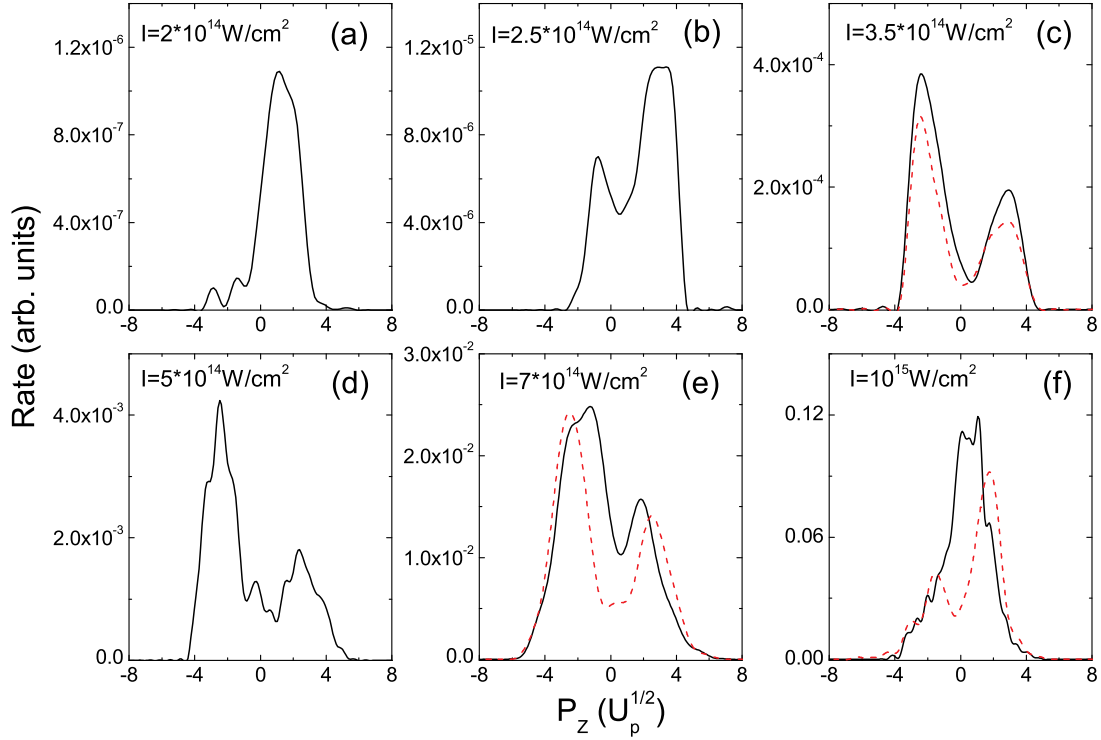


Figure 2: (Color on line) Momentum distribution of He^{2+} parallel to the polarization of the laser field with $\varphi_0 = 0$ and $I = 2.0 \times 10^{14} \text{ W/cm}^2$ (a), $2.5 \times 10^{14} \text{ W/cm}^2$ (b), $3.5 \times 10^{14} \text{ W/cm}^2$ (c), $5 \times 10^{14} \text{ W/cm}^2$ (d), $7 \times 10^{14} \text{ W/cm}^2$ (e), and $1 \times 10^{15} \text{ W/cm}^2$ (f). The dashed curve in (c), (e), and (f) is the momentum distribution of He^{2+} without the laser field during the recollision of e_1 .

- [5] A. Huillier, L. A. Lompre, G. Mainfray and C. Manus, Phys. Rev. A. **27**, 2503 (1983).
- [6] A. Becker and F. H. M. Faisal, Phys. Rev. Lett. **89**, 193003 (2002); A. Jaron and A. Becker, Phys. Rev. A **67**, 035401 (2003).
- [7] C. Figueira de Morisson Faria, H. Schomerus, X. Liu and W. Becker, Phys. Rev. A **69**, 043405 (2004); D. B. Milosevic and W. Becker, Phys. Rev. A **68**, 065401 (2003); D. B. Milošević, G. G. Paulus, D. Bauer, and W. Becker, J. Phys. B **39**, R203 (2006).
- [8] J. Chen, J. Liu, L. B. Fu, W. M. Zheng, Phys. Rev. A. **63**, 011404(R) (2000); L. B. Fu, J. Liu, J. Chen, and S.-G. Chen, Phys. Rev. A. **63**, 043416 (2001).
- [9] J. Chen, J. H. Kim, and C. H. Nam, J. Phys. B **36**, 691 (2003).

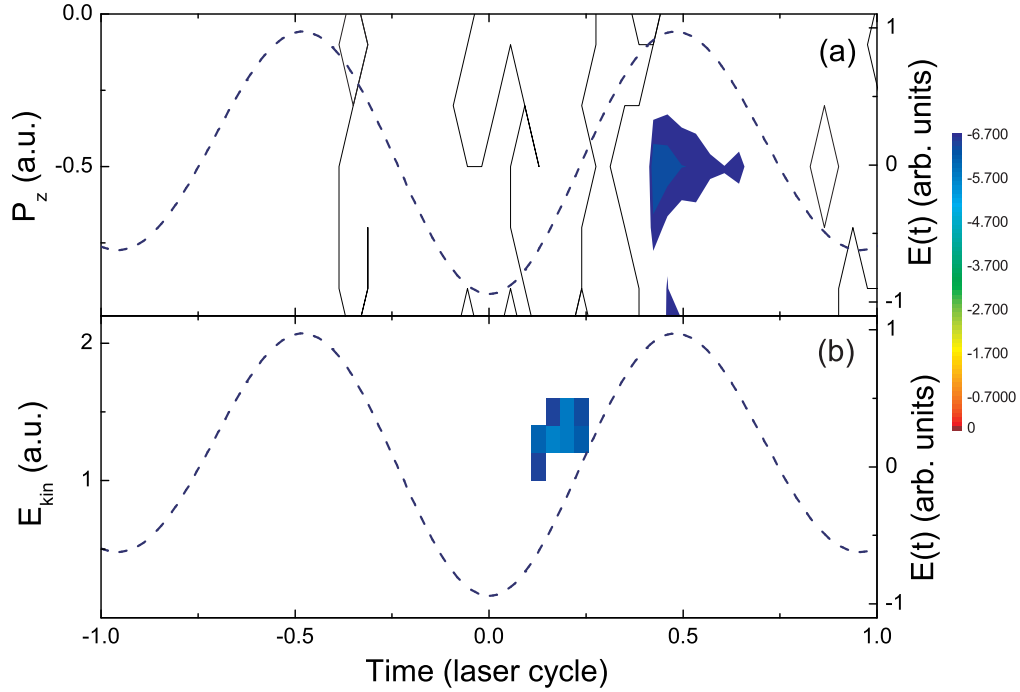


Figure 3: (Color on line) (a) The momentum distribution of He^{2+} parallel to the polarization of the laser field as a function of double ionization time with $\varphi_0 = 0$ when the peak intensity of the laser pulse is $I = 2.0 \times 10^{14} \text{ W/cm}^2$. (b) The corresponding kinetic energy distribution of the returning electron when it recollides with the ion. The laser field is also presented (the dashed curve). The results are plotted in log scale.

- [10] M. Yu. Kuchiev, JETP Lett. **45**, 404 (1987).
- [11] P. B. Corkum, Phys. Rev. Lett. **71**, 1994 (1993).
- [12] K. J. Schafer, B. Yang, L. F. DiMauro, and K. C. Kulander, Phys. Rev. Lett. **70**, 1599 (1993).
- [13] E. Eremina, X Liu, H Rottke, W Sandner, A Dreischuh, F Lindner, F Grasbon, G. G. Paulus, H. Walther, R. Moshhammer, B. Feuerstein, and J. Ullrich, J. Phys. B **36**, 3269 (2003).
- [14] B. Feuerstein, R. Moshhammer, and J. Ullrich, J. Phys. B **33**, L823 (2000).
- [15] A. Rudenko, Th. Ergler, K. Zrost, B. Feuerstein, V. L. B. de Jesus, C. D. Schroter, R. Moshhammer, and J. Ullrich, J. Phys. B **41**, 081006 (2008).

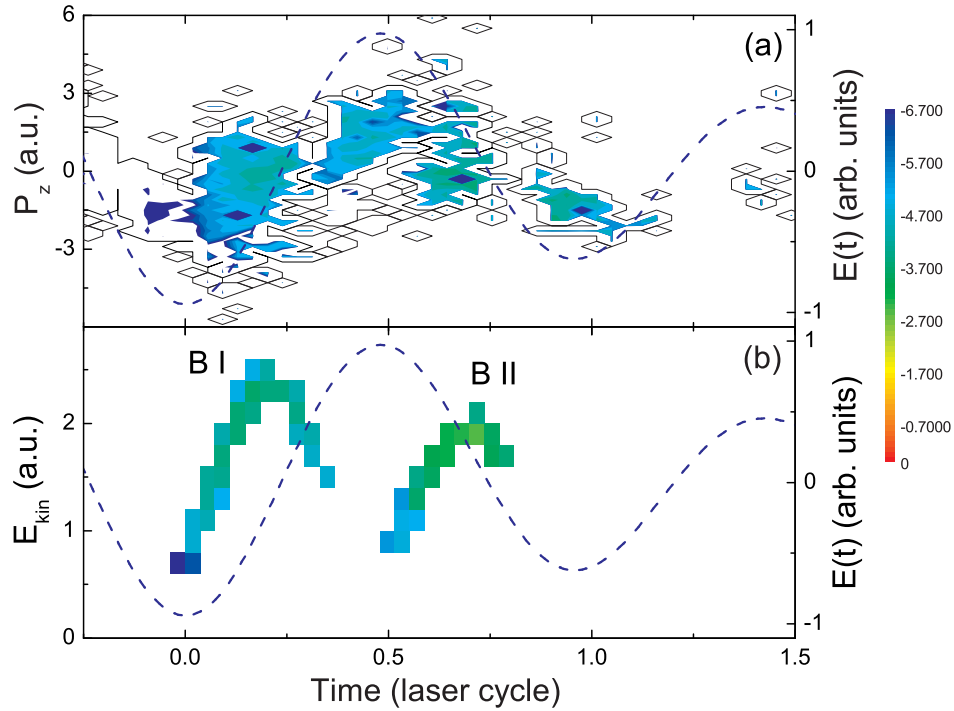


Figure 4: (Color on line) (a) Momentum distribution of He^{2+} parallel to the polarization of the laser field as a function of double ionization time with $\varphi_0 = 0$ when the peak intensity of the laser pulse is $I = 3.5 \times 10^{14} \text{ W/cm}^2$. (b) The corresponding kinetic energy distribution of the returning electron when it recollides with the ion. The laser field is also presented (the dashed curve). The results are plotted in log scale.

- [16] A. Rudenko, Th. Ergler, K. Zrost, B. Feuerstein, V. L. B. de Jesus, C. D. Schroter, R. Moshhammer, and J. Ullrich, *Phys. Rev. A* **78**, 015403 (2008).
- [17] Th. Weber, M. Weckenbrock, A. Staudte, L. Spielberger, O. Jagutzki, V. Mergel, F. Afaneh, G. Urbasch, M. Vollmer, H. Giessen, and R. Dorner, *J. Phys. B* **33**, L127 (2000).
- [18] O. Herrwerth, A. Rudenko, M. Kremer, V. L. B. de Jesus1, B. Fischer, G. Gademann, K. Simeonidis, A. Achtelik, T. Ergler, B. Feuerstein, C. D. Schroter, R. Moshhammer and J. Ullrich, *New J. Phys.* **10**, 025007 (2008).
- [19] M. V. Ammosov, N. B. Delone, and V. P. Krainov, *Sov. Phys. JETP* **64**, 1191 (1986).
- [20] J. S. Cohen, *Phys. Rev. A* **26**, 3008 (1982).

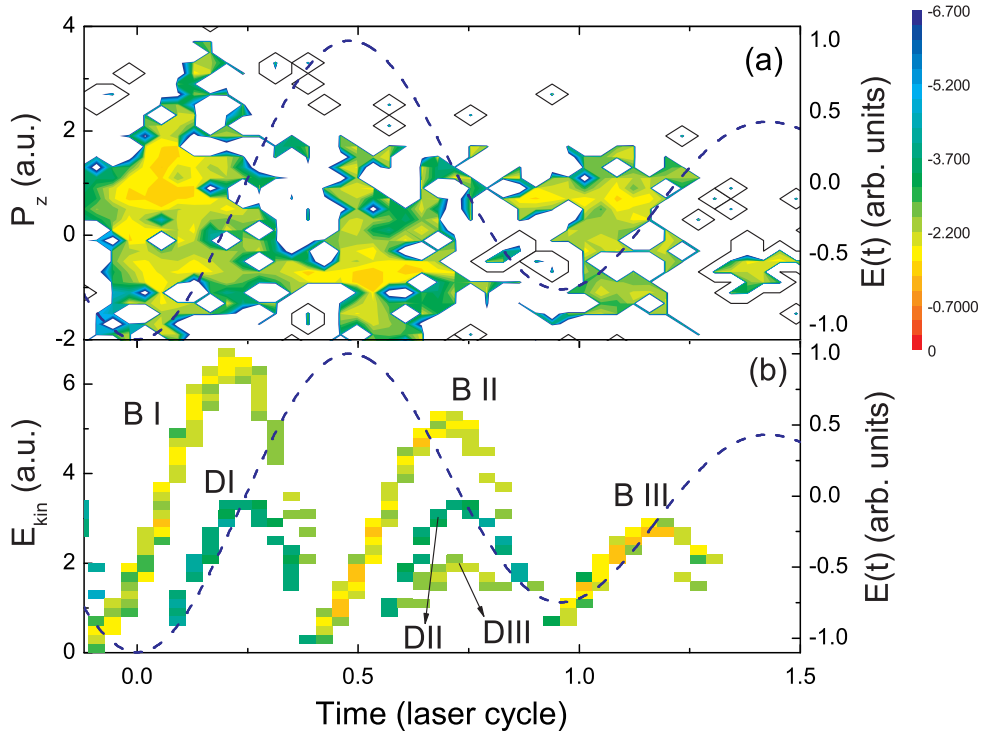


Figure 5: (Color on line) (a) The momentum distribution of He^{2+} parallel to the polarization of the laser field as a function of double ionization time with $\varphi_0 = 0$ when the peak intensity of the laser pulse is $I = 1 \times 10^{15} \text{ W/cm}^2$. (b) The corresponding kinetic energy distribution of the returning electron when it recollides with the ion. The laser field is also presented (the dashed curve) in (a) and (b). The results are plotted in log scale.

- [21] V. L. B. de Jesus, B. Feuerstein, K. Zrost, D. Fischer, A. Rudenko, F. Afaneh, C. D. Schroter, R. Moshhammer, and J. Ullrich, *J. Phys. B* **37**, L161 (2004).
- [22] H. Li, B. Wang, J. Chen, H. Jiang, X. Li, J. Liu, Q. Gong, Z.-C. Yan, and P. Fu, *Phys. Rev. A* **76**, 033405 (2007).
- [23] G. L. Yudin and M. Yu. Ivanov, *Phys. Rev. A* **63**, 033404 (2001).

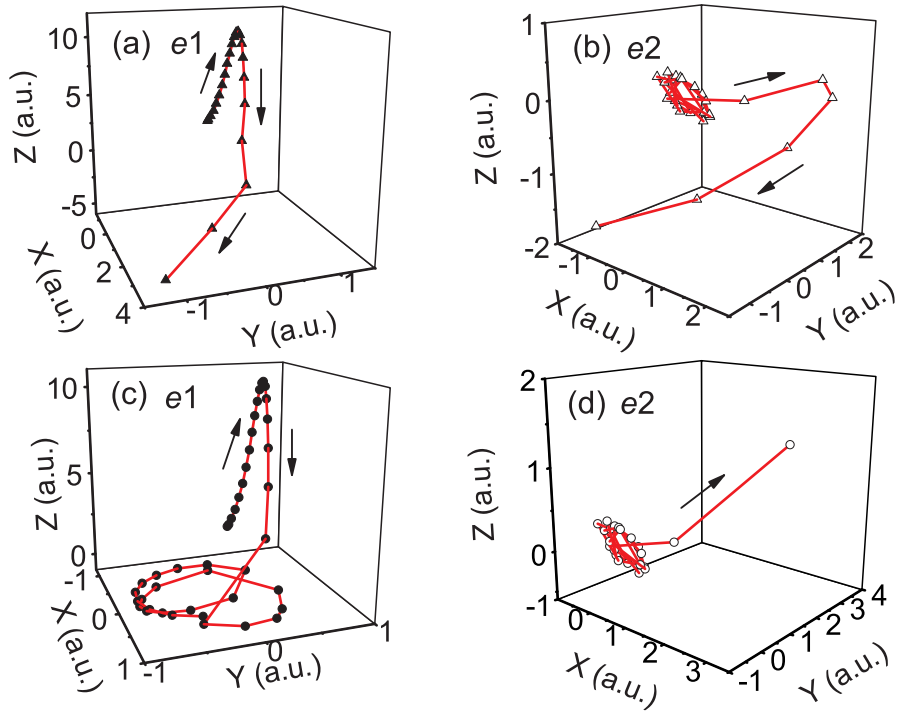


Figure 6: (Color on line) An LACI trajectory for e_1 (a) and e_2 (b) at $I = 1 \times 10^{15}$ W/cm². (c) and (d): The corresponding trajectories for e_1 and e_2 respectively without the laser field during the recollision. The arrow indicates the direction of a trajectory.

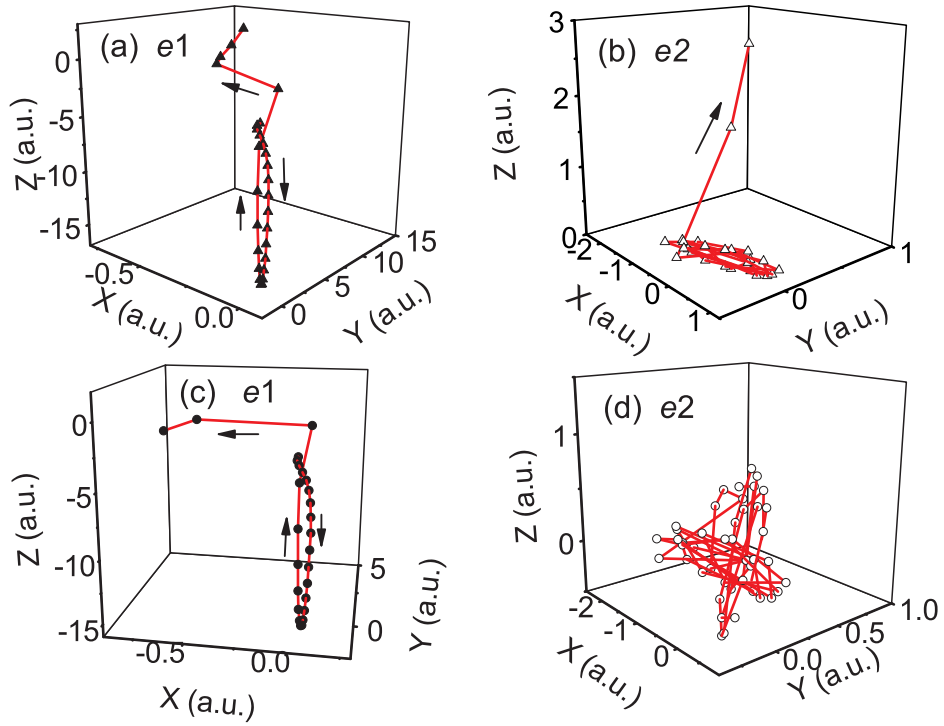


Figure 7: (Color on line) Another LACI trajectory for e_1 (a) and e_2 (b) at $I = 1 \times 10^{15}$ W/cm². (c) and (d): The corresponding trajectories for e_1 and e_2 respectively without the laser field during the recollision. The arrow indicates the direction of a trajectory.